International Journal of Emerging Trends & Technology in Computer Science (IJETTCS)
Web Site: www.ijettcs.org Email: editor@ijettcs.org, editorijettcs@gmail.com
Volume 10, Issue 2, March – April 2021 ISSN 2278-6856

AFast Image Super-Resolution Algorithm Based on Bilateral 4 Degree Interpolation

Gengyi Liu

School of Information Science and Engineering, Southeast University
Nanjing211189, China

Abstract:*As one of the effective methods, image interpolation is often used toestimatethe high-resolution (HR) images from the low-resolution (LR) images, how to construct the fast image interpolation algorithm becomes one of the problems that must be solved in practical application. A bilateral 4degree (Bi4D) interpolation is proposed to estimate the HR image of the LR image. The interpolation region [i-2,i+2] is translated into the region [-2,2]×[-2,2], and the pixel values of the translated region are invariant corresponding to the interpolation region. Similarly, the compensated pixel region [i,i+1]×[j,j+1] is translated into the region [0,1]×[0,1]. Experimental results show that the Bi4D methods achieve better performance than that of the traditional interpolation-based and learning-based image super-resolution methods.*

Keywords: Bi4D, bicubic interpolation, low-resolution, high-resolution

1. INTRODUCTION

Image information is one of the most important information obtained by humanbeings[1]. Image acquisition is the core technology of the digital camera, videophone, multimedia IP phone and teleconference, and plays an important role in modern multimedia technology. The speed and quality of image acquisition directly affect the overall effect of the productin digital image processing, image recognition and other fields[2,3,4].Image sensor is one of the main tools to sense the surrounding image information.

There are two kinds of common image sensors: CCD and CMOS[5,6]. At present, CCD still occupies the main position in the market, and with the development of CMOS technology, CMOS sensors have been widely used. The advantages of CCD are high sensitivity, small pixel, low reading noise, large dynamic range, so it occupies the main position in the field of solid-state imaging.

For optical imaging system, high resolution can provide more details in the same field of view. Both CCD and CMOS chips are developing towards high resolution. One of the ways to improve the resolution is to increase the size of the chip crystal, and the other is to reduce the size of the pixel, so as to obtain more image pixels on the same area of crystal. However, the trend of increasing camera resolution by reducing pixel size is not unlimited, because the smaller the pixel size, the higher the requirements of optical lens, and the more complex the chip production process, the higher the production cost [7].

Image is the offspring that people apperceive in the surrounding world and one of the most common and most extensive data types in the real world. Image resolution directly affects the degree to which people recognize the object in the image. High-resolution (HR) images include more image details compared with low-resolution (LR) images. HR images are convenient for people to study the interest regions in images [8,9]. However, most images in the real world are LR images, such as images taken by mobile phones. On the one hand, it is easier for people to obtain LR images in daily life, on the other hand, LR images take up less bandwidth in network transmission and are easy to share with others. Therefore, how to reconstruct a corresponding HR image from an LR image is the hotspot of attention [10,11]. Each year, there are special conferences or competitions for super-resolution reconstruction or image enhancement [12,13].

The process of producing an HR image from a sequence of LR images or a single image is called image super-resolution (SR). In general, LR images are noisy, blurred, and downsampled, and in this paper, LR images refer to the downsampled images. In recent years, image super-resolution reconstruction has been applied to many fields of research such as medical imaging [14,15] and satellite image processing[16,17]. Currently, image SR mainly includes three methods, reconstruction [18,19], interpolation [20,21], and machine learning techniques [22].

Here, we mainly focus on the image interpolation SR approaches that have the property of low computational complexity. However, the image interpolation SR methods tend to produce results with artifacts, such as mean square error (MSE), power signal-to-noise ratio (PSNR), and structure similarity measure (SSIM), compared with real images due to degradation of the high-frequency components of the image [23].

In the traditional image interpolation SR algorithm, the generated HR image has obvious jagged edges and mosaic regions. The bilinear image interpolation SR algorithm has a smoothing function, which degenerates the high-frequency part of the image and blurs the image details. The image interpolation SR algorithm can make the interpolated pixel value continue to change the continuity of the original pixel value, so the HR images by interpolation methods are natural and smooth.

Pixel value mutation occurs between some adjacent pixels, that is, pixel value discontinuities exist. For pixels with discontinuous pixel values, the conventional interpolation

algorithm is applied to HR image by generating compensated pixel points and the corresponding compensated pixel values, the contour and texture of the HR image will be blurred, and the image quality will be reduced.

To overcome the shortcomings of traditional interpolation methods, some interpolation methods of edge protection are put forward to obtain better image enhancement visual effects. Two methods are proposed to improve the achieved HR images including the formation of the high-degree image interpolation algorithms and the construction of the image adaptive interpolation method according to the selected patch features, such as the pixel value variance of the patch.

In order to achieve the corresponding HR image of the LR image, the prior knowledge of the LR image, such as the pixel points, the pixel values, and the gradient of adjacent pixels, are used to form the mapping relation between the LR image and the corresponding HR image. In this paper, the pixel points and the pixel values are used to form the relation between LR image and HR image. The bilateral four degree (Bi4D) is constructed to improve the quality of the estimated HR image by the following two strategies: (1) Bi4D interpolation function is constructed by the prior knowledge of LR image, and (2) the compensated pixel values of compensated pixel points are estimated by the constructed Bi4D interpolation function. We compared the proposed method with the traditional methods, such as bicubic interpolation image SR method andlearning–based image SR method, from the aspects MSE, PSNR, and SSIM.

2. BILATERAL 4 DEGREE INTERPOLATION

Digital image is stored in matrix form in computer, as far as gray image is concerned, the value V of the image corresponding matrix is the pixel value of the pixel point (i, j). Image interpolation is a technique that improves the resolution of the image by estimating the pixel values of the compensated pixel points.

2.1Construction of Bilateral 4 Degree Interpolation

For 3-dimensional space composed by the pixel points and the corresponding pixel values, the interpolation is to construct the relation between the input in 2-dimensional space composed of the pixel points in plane and the output in 1-dimensional space composed by the pixel values, the 2-dimensional space is denoted by the X-axis and Y-axis of pixel points, and the 1-dimensional space is denoted by the pixel values. In the other words, the image interpolation is to construct the following binary function to estimate the pixel values of the compensated pixel points.

$$f(x,y)=\sum_{s=0}^{4}\sum_{t=0}^{4}a_{st}x^{s}y^{t} \quad (1)$$

x and y are inputs, $f(x,y)$ is output, a_{st} are the parameters. For image interpolation, the binary function is used to predict the pixel value of the compensated pixel points. For the given image, the pixel points and their corresponding pixel values are known, the interpolation methods are used to determine the parameters a_{st} of the formula (1) which has 25 parameters. It is necessary that there are 25 pixel points and the corresponding pixel values to determine the 25 parameters.

For the given LR image I_0 with the size $m\times n$, the interpolation region of the pixel point (i,j) is $[i-2,i+2]\times[j-2,j+2]$ shown in Figure 1(a), and the corresponding pixel valuesare $V(x,y)$ x and y are integers on X-axis and Y-axis in the interpolation region. The interpolation region and the corresponding values are selected to form the interpolation formula (1). There are 25 pixel points and the corresponding pixel values for the pixel point (i,j). For the LR image, the Bi4D interpolation formula has the following general form.

$$V(x,y)=\sum_{s=0}^{4}\sum_{t=0}^{4}a_{st}x^{s}y^{t} \quad (2)$$

Where x and y are integers in the interpolation region, $V(x,y)$ is the corresponding pixel values, $a_{st}$are the parametersdetermined by the pixel points falling on the interpolation region and the corresponding pixel values.

The key of constructing Bi4D interpolation function is the determination of the parameter a_{st} in formula (2). In order to construct a unified interpolation form, the interpolation region is translated into the region $[-2,2]\times[-2,2]$ shown in Figure 1(b), and the interpolation function is transformed into the following function.

$$V(x,y)=\sum_{s=0}^{4}\sum_{t=0}^{4}a_{st}(x-i)^{s}(y-j)^{t} \quad (3)$$

Compared with the function (2), the function (3) maps the interpolation region $[i-2,i+2]\times[j-2,j+2]$ into the interpolation region $[-2,2]\times[-2,2]$ bythe shift $(x-i,y-j)$. For the different interpolation regions $[i-2,i+2]\times[j-2,j+2]$ of the pixel points (i,j), the right terms of function (3) have the same forms, and pixel values $V(x,y)$ are different for the interpolation regions corresponding to the different pixel points. Therefore, the parameters a_{st} of interpolation function are determined by the pixel values $V(x,y)$ for the different interpolation regions.

(a)

(i − 2, j − 2)	(i − 2, j − 1)	(i − 2, j)	(i − 2, j + 1)	(i − 2, j + 2)
(i − 1, j − 2)	(i − 1, j − 1)	(i − 1, j)	(i − 1, j + 1)	(i − 1, j + 2)
(i, j − 2)	(i, j − 1)	(i, j)	(i, j + 1)	(i, j + 2)
(i + 1, j − 2)	(i + 1, j − 1)	(i + 1, j)	(i + 1, j + 1)	(i + 1, j + 2)
(i + 2, j − 2)	(i + 2, j − 1)	(i + 2, j)	(i + 2, j + 1)	(i + 2, j + 2)

(b)

(−2, −2)	(−2, −1)	(−2, 0)	(−2, 1)	(−2, 2)
(−1, −2)	(−1, −1)	(−1, 0)	(−1, 1)	(−1, 2)
(0, −2)	(0, −1)	(0, 0)	(0, 1)	(0, 2)
(1, −2)	(1, −1)	(1, 0)	(1, 1)	(1, 2)
(2, −2)	(2, −1)	(2, 0)	(2, 1)	(2, 2)

Figure 1 The translation of the interpolation region. (a) the

interpolation region. (b)the translated interpolation region.

For the interpolation region shown in Figure 1, the key issueis to determine the values of parameters a_{st} in function (3). For each $(x-i, y-j) \in [-2,2]\times[-2,2]$ and $V(x,y)$, the function (3) is regarded as the linear equation with the variables a_{st}, for the interpolation region $[i-2,i+2]\times[j-2,j+2]$, there is the linear equation system.

$$T_1 a = V \tag{4}$$

Where T_1 is the coefficient matrix induced by $(x-i)^s(y-j)^t$, s=0,1,2,3,4, t=0,1,2,3,4, a is a vector composed of a_{st}, and V is a vector composed of $V(x,y)$. T1 is constant, the parameter a is determined by the different pixel values V for the different interpolation regions $[i-2,i+2]\times[j-2,j+2]$. The parameter a is computed by the following formula.

$$a = T_1^{-1}V$$

where T_1^{-1} is the inverse matrix of the coefficient matrix T_1. So we achieve the following image interpolation function (5) which is used to predict the pixel values of the compensated pixel points in the compensation region $[i,i+1]\times[j,j+1]$.

$$S = (T_1^{-1}V)^T T_2 \tag{5}$$

Where T_2 is the pixel compensation matrix determined by $(x-i)^s(y-j)^t$ (s=0,1,2,3,4, t=0,1,2,3,4) in the pixel compensation region $[i,i+1]\times[j,j+1]$, namely $(x,y)\in[i,i+1]\times[j,j+1]$ where (x,y) is the pixel compensation point.

The formula (5) is a bilateral function because both sides of V are constants, $T_1^{-1}$is determined by the interpolation region $[i-2,i+2]\times[j-2,j+2]$ which has been transformed into the region $[-2,2]\times[-2,2]$, and T_2 is determined by the compensation pixel region $[i,i+1]\times[j,j+1]$ which has been transformed into the region $[0,1]\times[0,1]$. For the different compensation pixel points, the different compensated pixel values are determined by the pixel value of pixel points lying in the interpolation region $[i-2,i+2]\times[j-2,j+2]$ and the compensation pixel region $[i,i+1]\times[j,j+1]$.

2.2 Image Super-resolution Based on Bilateral 4 Degree Interpolation

The image interpolation SR reconstructs the HR image by the compensated pixel method, which predicts the pixel values of the compensated pixel points by the interpolation function (5) formed by the interpolation region for the LR image.

For the pixel point (i,j), we compensate the pixel values in the compensation region $[i,i+1]\times[j,j+1]$ by the interpolation function in the region $[i-2,i+2]\times[j-2,j+2]$. For the SR factor M, the compensated imagepatch with the size $(M-1)\times(M-1)$ is constructed in the region $[i,i+1]\times[j,j+1]$to replace the pixel point (i,j). To obtain the compensatedimage patch, the region $[i,i+1]\times[j,j+1]$ is divided into the $M\times M$ grid, and the coordinates of the grid points are $(i+p/M, j+q/M)$,p=0,1,…,M,q=0,1,…,M, shown in Figure 2(a) when M=4. In practically, the compensation region is translated into the region $[0,1]\times[0,1]$shown in Figure 2(b) when M=4.Thecompensated pixelvalues are computed by the constructed interpolation function (5).

(a)

(i, j)	(i, j + 0.25)	(i, j + 0.5)	(i, j + 0.75)	(i, j + 1)
(i + 0.25, j)	(i + 0.25, j + 0.25)	(i + 0.25, j + 0.5)	(i + 0.25, j + 0.75)	(i + 0.25, j + 1)
(i + 0.5, j)	(i + 0.5, j + 0.25)	(i + 0.5, j + 0.5)	(i + 0.5, j + 0.75)	(i + 0.5, j + 1)
(i + 0.75, j)	(i + 0.75, j + 0.25)	(i + 0.75, j + 0.5)	(i + 0.75, j + 0.75)	(i + 0.75, j + 1)
(i + 1, j)	(i + 1, j + 0.25)	(i + 1, j + 0.5)	(i + 1, j + 0.75)	(i + 1, j + 1)

(b)

(0, 0)	(0, 0.25)	(0, 0.5)	(0, 0.75)	(0, 1)
(0.25, 0)	(0.25, 0.25)	(0.25, 0.5)	(0.25, 0.75)	(0.25, 1)
(0.5, 0)	(0.5, 0.25)	(0.5, 0.5)	(0.5, 0.75)	(0.5, 1)
(0.75, 0)	(0.75, 0.25)	(0.75, 0.5)	(0.75, 0.75)	(0.75, 1)
(1, 0)	(1, 0.25)	(1, 0.5)	(1, 0.75)	(1, 1)

Figure 2 The translation of compensation region. (a) the compensation region. (b) the translated compensation region.

For the LR image, we reconstruct the corresponding HR image by the following algorithm.

Algorithm1. Bi4D algorithm
Input: LR image L with size m×n, SR factor M
Output: corresponding HR image H
S1. L1=[L(1,:);L(1,:);L;L(end,:);L(end,:)];
L2=[L1(:,1) L1(:,1) L1 L1(:,end) L1(:,end)];
S2. [m,n]=size(L2)
S3. Id0 = 0;
S4. For k2=1:5
S5. For k1=1:5
S6. Id0 = id0+1;
S7. Tm0(:,:,id0) = L2(k1:k1+m-5,k2:k2+n-5);
S8. End for k1
S9. End for k2
S10. Tm1=permute(Tm0,[3,1,2]);
S11. v=reshape(Tm1,5*5,size(Tm0,1)*size(Tm0,2));
S12. Compute T2 in the pixel compensation region [i,i+1]×[j,j+1].
S13. S=(T1-1v)TT2
S14. for t1 = 1:M
S15. for t2 = 1:M
S16. H(t1:M:M*m,t2:M:M*n)=reshape(S(t1*(t2-1)+1,:),m,n);
S17. End for t2
S18. End for t1

The Bi4D algorithm constructs the corresponding HR image for the LR image with only one channel, such as the gray image. For the other image, such as RGB image, the Bi4D algorithm is performed on each channel. The aim of Bi4D algorithm is to construct bilateral 4 degree interpolation surfaces in interpolation regions to estimate the pixel value in the compensation regions.

In Bi4D algorithm, T_1 is determined by $(x-i)^s(y-j)^t$ (s=0,1,2,3,4, t=0,1,2,3,4) where both x and y are integers and belong to the interpolation region

$[i-2,i+2]\times[j-2,j+2]$, and T_2 is determined by $(x-i)^s(y-j)^t$ (s=0,1,2,3,4, t=0,1,2,3,4) where $x=i+p/M$ and $y=j+q/M$ belong to the compensation region $[i,i+1]\times[j,j+1]$ $p=0,1,2,...,M$, $q=0,1,2,...,M$. Therefore, for a certain SR factor M, T_1 and T_2 are determined.

In S1, the original LR image is extended to ensure that each pixel has the corresponding interpolation region, and L_2 is the extended LR image.

	1	2	3	4	5	6	7	8	9
1	32	68	72	42	63	21	61	36	39
2	40	16	62	28	8	25	50	71	13
3	22	69	70	17	67	52	26	23	9
4	34	11	51	41	59	37	43	65	66
5	35	54	33	47	5	64	19	2	20
6	6	30	7	14	48	31	44	4	57
7	55	45	38	46	53	49	15	18	10
8	3	60	58	56	29	27	1	24	12

Figure 3 Example extended image with size 8×9

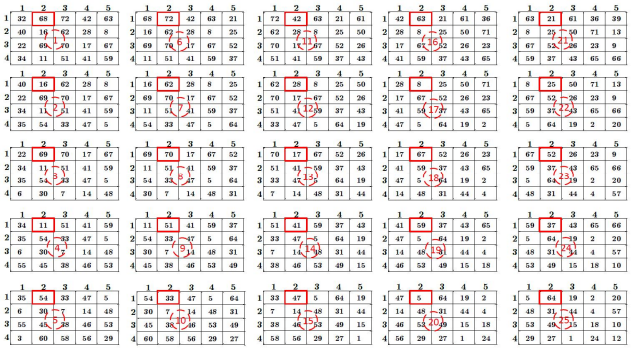

Figure 4 The fast extraction of pixel values by Bi4D algorithm

In S7, the 25 pixel values in interpolation region $[i-2,i+2]\times[j-2,j+2]$ are extracted at one time. An example is given to illustrate the extraction process. For the extended image with the size 8×9 ($m=8$, $n=9$ in Bi4D algorithm), when $i=3$, $j=4$, the pixel point $(3,4)$ is marked in red lines in Figure 3, all the 25 pixel points lie in the interpolation region marked in the blue lines in Figure 3, and the corresponding pixel values are shown in determined locations marked in the red rectangle of the sub-images from 1 to 25 shown Figure 4 which are induced by example extended image shown in Figure 3. All the sub-images are transformed into vectors, 25 vectors are generated for the image shown in Figure 3. The corresponding vector of pixel point (3,4) is[68,16,69,11,54,72,62,70,51,33,42,28,17,41,47,63,8,67,59 ,5,21,25,52,37,64]^T shown in Figure 5.

As mentioned above, for a certain SR factor M, T_1 and T_2 are determined by the interpolation region $[i-2,i+2]\times[j-2,j+2]$ and the compensation region $[i,i+1]\times[j,j+1]$, T_1 is computed by $(x-i)^s(y-j)^t$ (s=0,1,2,3,4, t=0,1,2,3,4) where x and y are integers lying in the interpolation region $[i-2,i+2]\times[j-2,j+2]$, and T_2 is determined by $(x-i)^s(y-j)^t$ (s=0,1,2,3,4, t=0,1,2,3,4) where (x,y) is the compensated pixel points with values in the compensation region $[i,i+1]\times[j,j+1]$. The transposition of matrix S has the following form shown in Figure 6 for S13 when $M=2$ for the image shown in Figure 3. The pixel point (3,4) is replaced by the image patch [17 32.0313;27.0781 39.7787] induced by the raw marked in red lines in Figure 6.

32	40	22	34	68	16	69	11	72	62	70	51	42	28	17	41	63	8	67	59
40	22	34	35	16	69	11	54	62	70	51	33	28	17	41	47	8	67	59	5
22	34	35	6	69	11	54	30	70	51	33	7	17	41	47	14	67	59	5	48
34	35	6	55	11	54	30	45	51	33	7	38	41	47	14	46	59	5	48	53
35	6	55	3	54	30	45	60	33	7	38	58	47	14	46	56	5	48	53	29
68	16	69	11	72	62	70	51	42	28	17	41	63	8	67	59	21	25	52	37
16	69	11	54	62	70	51	33	28	17	41	47	8	67	59	5	25	52	37	64
69	11	54	30	70	51	33	7	17	41	47	14	67	59	5	48	52	37	64	31
11	54	30	45	51	33	7	38	41	47	14	46	59	5	48	53	37	64	31	49
54	30	45	60	33	7	38	58	47	14	46	56	5	48	53	29	64	31	49	27
72	62	70	51	42	28	17	41	63	8	67	59	21	25	52	37	61	50	26	43
62	70	51	33	28	17	41	47	8	67	59	5	25	52	37	64	50	26	43	19
70	51	33	7	17	41	47	14	67	59	5	48	52	37	64	31	26	43	19	44
51	33	7	38	41	47	14	46	59	5	48	53	37	64	31	49	43	19	44	15
33	7	38	58	47	14	46	56	5	48	53	29	64	31	49	27	19	44	15	1
42	28	17	41	63	8	67	59	21	25	52	37	61	50	26	43	36	71	23	65
28	17	41	47	8	67	59	5	25	52	37	64	50	26	43	19	71	23	65	2
17	41	47	14	67	59	5	48	52	37	64	31	26	43	19	44	23	65	2	4
41	47	14	46	59	5	48	53	37	64	31	49	43	19	44	15	65	2	4	18
47	14	46	56	5	48	53	29	64	31	49	27	19	44	15	1	2	4	18	24
63	8	67	59	21	25	52	37	61	50	26	43	36	71	23	65	39	13	9	66
8	67	59	5	25	52	37	64	50	26	43	19	71	23	65	2	13	9	66	20
67	59	5	48	52	37	64	31	26	43	19	44	23	65	2	4	9	66	20	57
59	5	48	53	37	64	31	49	43	19	44	15	65	2	4	18	66	20	57	10
5	48	53	29	64	31	49	27	19	44	15	1	2	4	18	24	20	57	10	12

Figure 5 Vectors by all the pixel points for example image S16 is designed to realize the fast procedure that vectors are transformed into image patches and regarded as the inverse procedure of S7.

70	62.5391	45.2734	45.7944
51	41.7578	46	45.0494
33	19.8828	40.6563	26.1896
7	3.9688	8.6797	4.558
17	27.0781	32.0313	39.7787
41	48.0547	48.2656	41.8658
47	33.0547	28.5078	26.2317
14	9.4766	30.2031	30.8914
67	65.6719	69.4531	62.9321
59	33.0547	51.9375	37.8372
5	16.4922	26.2031	31.0745
48	54.9766	44.5391	47.8775
52	44.5	37.6641	36.3759
37	47.8984	36.2344	44.236
64	53.7578	53.4844	47.2383
31	25.9844	33.5312	30.4769
26	34.2422	22.8984	33.376
43	33.9688	44.3125	31.7708
19	26.1563	11.6406	21.617
44	47.8828	46.125	51.4707

Figure 6 The vectors by the compensated pixel values

3 EXPERIMENTS

To verify the performance of Bi4D algorithm proposed in the paper, we select the benchmark image sets named BSD300[24] and B100[12,13] to compare the image interpolation algorithms, such as Bi4D interpolation algorithm and bilateral cubic (bicubic) interpolation algorithm. We also compare Bi4D interpolation algorithm with the learning-based algorithms, such as ANR[25], A+[26], and NE+LLE[27]. ANR (Anchored Neighborhood Regression) is among the fastest known super-resolution methods. ANR learns sparse dictionaries and regressors anchored to the dictionary atoms. A+ is an improved variant of ANR, which combines the best qualities of ANR and SF (Simple Functions). SF relies on clusters and corresponding learned functions.

The performance of SR algorithms includes the MSE (Mean Squared Error), PSNR (Peak Signal to Noise Ratio), and SSIM (Structure Similarity) between the HR image and the interpolated HR image[23,28].

Firstly, the selected images are regarded as the original HR images, and the corresponding LR images with size $m \times n$ are obtained by the following downsample formula

$$im = I(1:M:m,1:M:n,:) \quad (6)$$

where M is the SR factor.

Secondly, im is taken as the input, and the fast Bi4D algorithm is performed to obtain the interpolated HR image.

Thirdly, the interpolated HR image quality assessment indices, such as MSE, PSNR, SSIM, are computed.

3.1 Comparison of Bi4D and bicubic interpolation

The Bi4D superiority is demonstrated by the benchmark image sets, BSD300 includes 300 images, B100 includes 100 images. Each image is regarded as the original HR image, the corresponding LR image is downsampled by formula (6) to take as the input of Bi4D and bicubic algorithms, and the interpolated HR image is obtained by the performed Bi4D and bicubic algorithms.

The interpolated HR image quality assessment indices on the two image sets are listed inTable 1, from the table, we can see both the minimal MSE (min), the maximal MSE (max), and the mean MSE (mean) of Bi4D are less than those of bicubic, this shows that Bi4D algorithm is superior to bicubic algorithm for the MSE index. From the other two evaluation indices, PSNR and SSIM, we can draw the same conclusion as the index MSE, namely Bi4D is superior to bicubic algorithm from the indices, MSE, PSNR, and SSIM.

We compare the performance of each image in the two image sets from the image quality assessment indices, MSE, PSNR, and SSIM.We find that the Bi4D is superior to the bicubic algorithm for single image. Figure 7 shows the assessment indices PSNR and SSIM, the PSNRs of HR images by Bi4D are greater than those of bicubic, the SSIMs of HR images by Bi4D are greater than those of bicubic.

Therefore, the performance of Bi4D is better than that of bicubic in both image set and single image, namely Bi4D is superior to the traditional interpolation-based algorithm.

Table1: The MSE comparison of Bi4D and Bicubic image interpolation algorithms

Factors	Data sets	Alg.	min	max	mean
M=2	BSD300	Bi4D	2.0927	306.5907	50.8182
		Bicubic	3.7853	408.4834	71.9085
	B100	Bi4D	3.4217	250.3145	54.4646
		Bicubic	6.0395	309.2459	75.6358
M=3	BSD300	Bi4D	4.6384	580.0407	100.1652
		Bicubic	8.2378	741.6933	142.0525
	B100	Bi4D	8.1159	426.4157	104.7929
		Bicubic	14.2880	516.9646	146.8956
M=4	BSD300	Bi4D	7.2864	758.0857	136.4607
		Bicubic	10.6780	940.8795	192.9060
	B100	Bi4D	12.9656	526.1992	141.4935
		Bicubic	23.7920	637.7725	198.6888

Table2: The PSNR comparison of Bi4D and Bicubic image interpolation algorithms

Factors	Data sets	Alg.	min	max	mean
M=2	BSD300	Bi4D	18.4940	40.1525	27.8259
		Bicubic	17.2478	37.5786	26.0709
	B100	Bi4D	19.3747	38.0171	27.3972
		Bicubic	18.4566	35.5496	25.7089
M=3	BSD300	Bi4D	15.7250	36.6959	24.7214
		Bicubic	14.6573	34.2015	22.9750
	B100	Bi4D	17.0613	34.2662	24.3822
		Bicubic	16.2250	31.8099	22.6829
M=4	BSD300	Bi4D	14.5624	34.7344	23.2744
		Bicubic	13.6243	33.0747	21.5596
	B100	Bi4D	16.1481	32.2317	22.9753
		Bicubic	15.3129	29.5953	21.3015

Table3: The SSIM comparison of Bi4D and Bicubic image interpolation algorithms

Factors	Data sets	Algorithms	min	max	mean
M=2	BSD300	Bi4D	0.5129	0.9864	0.8407
		Bicubic	0.4395	0.9801	0.7907
	B100	Bi4D	0.5129	0.9803	0.8282
		Bicubic	0.4395	0.9738	0.7758
M=3	BSD300	Bi4D	0.3058	0.9714	0.7180
		Bicubic	0.2404	0.9649	0.6438
	B100	Bi4D	0.3058	0.9621	0.6996
		Bicubic	0.2404	0.9497	0.6225
M=4	BSD300	Bi4D	0.2276	0.9624	0.6437
		Bicubic	0.1777	0.9562	0.5671
	B100	Bi4D	0.2276	0.9474	0.6228
		Bicubic	0.1777	0.9327	0.5433

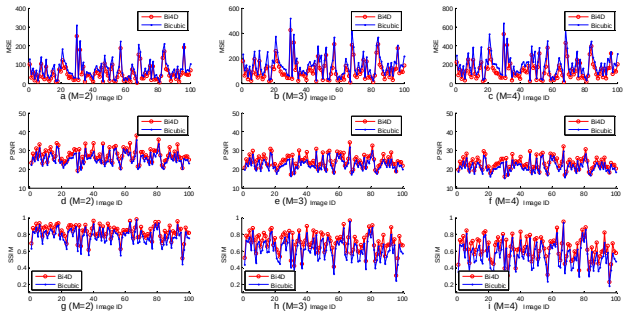

Figure 7 The comparison of Bi4D and Bicubic on the image set B100

3.2 Comparison of Bi4D and learning-based algorithms

We compare Bi4D image interpolation algorithms with the state-of-the-art image super resolution algorithms based on learning, such as ANR, A+, and NE+LLE. Table 4 shows the performances of PSNRs performed by Bi4D and the learning-based algorithms, the performance includes minimal PSNR, maximal PSNR, mean PSNR, and the standard deviation of PSNR. From the table 4, we can see Bi4D image interpolation algorithm achieves the better PSNR compared with the learning-based algorithms, such as ANR, NE+LLE, and A+.The PSNR in the references [25-27] is higher than that in the paper because the downsampling formula (9) in this paper does not utilize any

prior knowledge of HR images, while the nearest neighbor downsampling method in the references utilizes the prior knowledge of HR images, such as the nearest neighbor pixel points of the selected pixel point. In practical application, the HR image of the LR image is unknown, and we can not get the LR image of HR image by the nearest neighbor downsampling.So the downsampling method by formula (9) is reasonable for applications.

Table 4: Comparison of PSNRs performed by Bi4D and learning-based algorithms

Factors	Algorithms	min	max	mean
M=2	Bi4D	19.3563	37.9952	27.3838
	ANR	17.7081	35.0088	25.0519
	NE+LLE	18.4342	35.5098	25.6822
	A+	17.5431	34.8898	24.8967
M=3	Bi4D	17.0355	34.2141	24.3643
	ANR	15.5937	31.2367	22.0845
	NE+LLE	16.1983	31.7475	22.6639
	A+	15.4516	31.0834	21.9295
M=4	Bi4D	16.1071	32.1232	22.9620
	ANR	14.6523	28.9438	20.6970
	NE+LLE	15.2773	29.4812	21.2859
	A+	14.5230	28.7924	20.5598

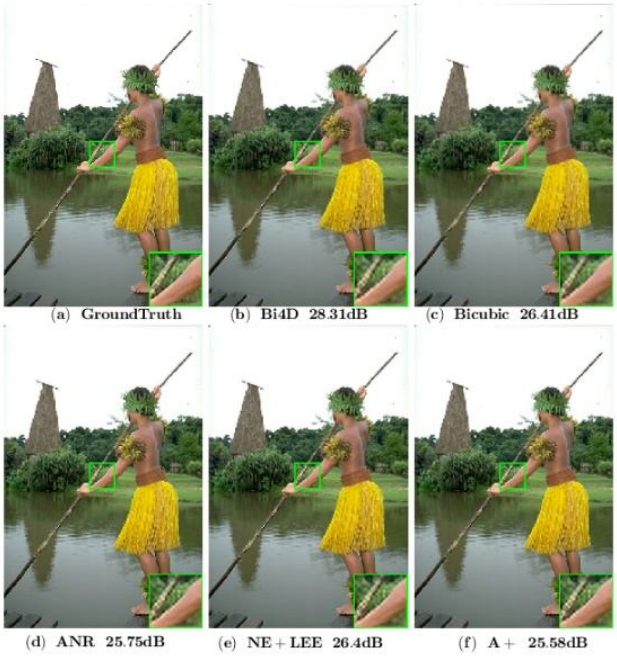

Figure 8 HR images of the images in image set B100 by different methods when M=2.

Figure 9 HR images of the images in image set B100 by different methods when M=3.

Figure 8 shows the constructed HR images of the images in image set B100 when image SR factor M=2, Figure 9 shows the constructed HR images of the images in image set B100 when image SR factor M=3, Figure 10 shows the constructed HR images of the images in image set B100 when image SR factor M=4. One can see that the Bi4D method results in not only higher PSNR measure, but also much better visual quality than other learning-based methods. Due to limited space, we do not show the results of all the images in visual quality comparison.

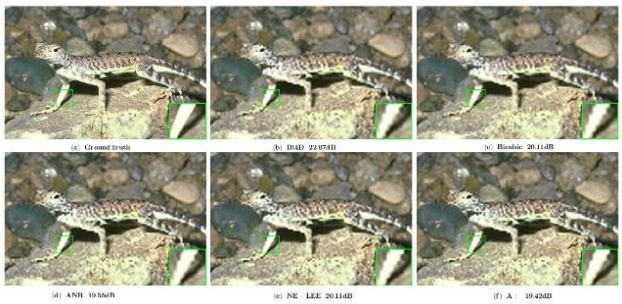

Figure 10 HR images of the images in image set B100 by different methods when M=4.

4 CONCLUSIONS

In this paper, we propose Bi4D image interpolation algorithm which estimate the corresponding HR image for the given LR image without the learning process. The experimental results demonstrate the superiority and feasibility of the Bi4D image interpolation method. Compared with the traditional bicubic interpolation image super-resolution algorithm, the Bi4D achieved better performances, such as MSE and PSNR. Compared with learning-based method, Bi4D without the training process saves running time.

Funding: This work was supported in part by the Student Research Training Program of Southeast University (202006063, 202104068).

References

[1] H.G. Kim,H. Lim,Y.M. Ro,"Deep virtual reality image quality assessment with human perception guider for omnidirectional image,"IEEE Transactions on Circuits and Systems for Video Technology, 30(4): 917-928, 2020.

[2] L. Graham,Y. Yitzhaky,"Blind restoration of space-variant Gaussian-like blurred images using regional PSFs," Signal, Image and Video Processing 13(4): 711-717, 2019.

[3] S. Wang,Y. Wang,H. Shang,C. Shi,"Multimodal computer image recognition based on depth neural network," Cluster Computing 22(6): 14819-14825, 2019.

[4] A. Marka,J. Carter,E. Toto, S.Hassanpour,"Automated detection of nonmelanoma skin cancer using digital images: a systematic review," BMC Medical Imaging 19(1): 21:1-21, 2019.

[5] X. Yin,G. Jiang,S. Song,"Research on an automatic tracking strategy based on CCD image sensor in micromanipulation," IEEE Access 6: 76374-76380, 2018.
[6] W. Kim,C. Park,H. Lee,I. Lee,B. Lee,"A high full well capacity CMOS image sensor for space applications," Sensors, 19(7): 1505, 2019.
[7] M.R.Elliott,D. Kim,D.S. Molony,L. Morris,H. Samady,S. Joshi,L.H. Timmins,"Establishment of an automated algorithm utilizing optical coherence tomography and Micro-Computed tomography imaging to reconstruct the 3-D deformed stent geometry," IEEE Transactions on Medical Imaging, 38(3): 710-720, 2019.
[8] H.G. Chen, X. He, M. Ma, L. Qing, Q. Teng,"Low bit rates image compression via adaptive block downsampling and super resolution," Journal of Electronic Imaging, 25(1): 01300401-10, 2016.
[9] S. Bonafoni, G. Tosi,"Downscaling of land surface temperature using airborne high-resolution data: a case study on aprilia, Italy," IEEE Geoscience Remote Sensing Letters, 14(1):107-111, 2017.
[10] P. Cheng, Y. Qiu, X. Wang, K. Zhao,"A new single image super-resolution method based on the infinite mixture model," IEEE Access, 5:2228-2240, 2017.
[11] C. Ma, C. Y. Yang, X. Yang, M.H. Yang,"Learning a no-reference quality metric for single-image super-resolution," Computer Vision and Image Understanding, 158:1-16, 2017.
[12] A. Abdelhamed,M. Afifi,R. Timofte,M.S. Brown, et al,"NTIRE 2020 Challenge on Real Image Denoising: Dataset, Methods and Results,"The IEEE Conference on Computer Vision and Pattern Recognition (CVPR) Workshops , June 2020.
[13] A. Lugmayr, M. Danelljan,R. Timofte, et al,"NTIRE 2020 Challenge on Real-World Image Super-Resolution: Methods and Results," In The IEEE Conference on Computer Vision and Pattern Recognition (CVPR) Workshops , June 2020.
[14] J. Song, H. Liu, K. Deng, C. Zhang,"Super resolution reconstruction of medical image based on adaptive quad-tree decomposition," Journal of Computation Methods in Science and Engineering, 17(3):411-422, 2017.
[15] Z. Lai, X. Qu, X. Liu, D. Guo, J. Ye, Z. Zhan,Z. Chen,"Image reconstruction of compressed sensing MRI using graph-based redundant wavelet transform," MedicalImage Analysis, 27:93-104, 2016.
[16] Y. Luo, L. Zhou, S. Wang, Z. Wang,"Video satellite imagery super resolution via convolutional neural networks," IEEE Geoscience Remote Sensing Letters, 14(12):2398-2402, 2017.
[17] Y. Yao, J. Han, G. Cheng, X. Qian, L. Guo,"Semantic annotation of high-resolution satellite images via weakly supervised learning," IEEE Transactions on Geoscience and Remote Sensing, 54(6):3660-3671, 2016.
[18] S. Huang, J, Sun, Y. Yang, Y. Fang, P. Lin,"Multi-frame super-resolution reconstruction based on gradient vector flow hybrid field," IEEE Access, 5:21669-21683, 2017.
[19] C. Singh, A. Aggarwal,"An efficient and robust multi-frame image super-resolution reconstruction using orthogonal Fourier-Mellin moments," Displays, 49:101-115, 2017.
[20] R.K. Lama, M.R. Choi, G.R. Kwon,"Image interpolation for high-resolution display based on the complex dual-tree wavelet transform and hidden Markov model," Multimedia Tools and Applications, 75(23):16487-16498, 2016.
[21] M. Sajjad, N. Ejaz, I. Mehmood, S.W. Baik,"Digital image super-resolution using adaptive interpolation based on Gaussian function," Multimedia Tools and Applications, 74(20):8961-8977, 2015.
[22] K. Zhang, D. Tao, X. Gao, X. Li, J. Li,"Coarse-to-fine learning for single-image super-resolution," IEEE Transactions on Neural Networks and Learning Systems, 28(5):1109-1122, 2017.
[23] Z. Wang,A.C. Bovik,H.R. Sheikh,E.P. Simoncelli,"Image quality assessment: from error visibility to structural similarity,"IEEE Transactions on Image Processing, 13(4):600–612, 2004.
[24] https://www2.eecs.berkeley.edu/Research/Projects/CS/vision/bsds/
[25] R. Timofte, V.D. Smet, L.J.V. Gool,"A+: adjusted anchored neighborhood regression for fast super-resolution," in Proc. ACCV, 2014.
[26] M. Bevilacqua,A. Roumy,C. Guillemot,M.L. Alberi-Morel,"Lowcomplexity single-image super-resolution based on nonnegative neighbor embedding,"in BMVC, 2012.
[27] H. Chang,D. Yeung,Y. Xiong,"Super-resolution through neighbor embedding,"in CVPR, 2004.
[28] C. Li,A.C. Bovik,"Content-partitioned structural similarity index for image quality assessment," Signal Processing: Image Communication, 25(7):517-526, 2010.

AUTHOR

Gengyi Liu, an undergraduate in School of Information Science and Engineering, Southeast University, Nanjing, China. His research interests include digital image processing, image reconstruction and image enhancement